

High-mobility transparent conductive Zr-doped In₂O₃

T. Koida and M. Kondo

Citation: *Applied Physics Letters* **89**, 082104 (2006); doi: 10.1063/1.2337281

View online: <http://dx.doi.org/10.1063/1.2337281>

View Table of Contents: <http://scitation.aip.org/content/aip/journal/apl/89/8?ver=pdfcov>

Published by the AIP Publishing

Articles you may be interested in

Transport properties of d-electron-based transparent conducting oxide: Anatase Ti_{1-x}Nb_xO₂

J. Appl. Phys. **101**, 093705 (2007); 10.1063/1.2721748

Comparative studies of transparent conductive Ti-, Zr-, and Sn-doped In₂O₃ using a combinatorial approach

J. Appl. Phys. **101**, 063713 (2007); 10.1063/1.2712161

Improved near-infrared transparency in sputtered In₂O₃-based transparent conductive oxide thin films by Zr-doping

J. Appl. Phys. **101**, 063705 (2007); 10.1063/1.2711768

Optically transparent and electrically conducting epitaxial Ta₂O₅ films

J. Appl. Phys. **101**, 063535 (2007); 10.1063/1.2495937

Investigation of transparent and conductive undoped Zn₂In₂O_{5-x} films deposited on n-type GaN layers

J. Appl. Phys. **92**, 274 (2002); 10.1063/1.1481207



High-mobility transparent conductive Zr-doped In_2O_3

T. Koida^{a)} and M. Kondo

Research Center for Photovoltaics, National Institute of Advanced Industrial Science and Technology (AIST), Central 2, Umezono 1-1-1, Tsukuba, Ibaraki 305-8568, Japan

(Received 11 April 2006; accepted 28 June 2006; published online 24 August 2006)

Optical and electric properties in Zr-doped In_2O_3 epitaxial layers were systematically investigated. The films at Zr concentrations of 0.3–0.5 at. % are found to be superior transparent conductive oxides in transparency in near infrared wavelength region and Hall mobility compared to Sn-doped In_2O_3 . Maximum mobilities are over $100 \text{ cm}^2/\text{V s}$ and corresponding carrier densities are approximately $1 \times 10^{20} \text{ cm}^{-3}$. From the relationship between the values of Hall mobility and carrier concentration of the epilayers, a number and/or effects of multicharged and neutral scattering centers of electrons seem to be reduced. © 2006 American Institute of Physics. [DOI: 10.1063/1.2337281]

Transparent conductive oxides (TCOs) having low resistivity¹ and high mobility^{2–6} are attracting attention, due to the rapidly rising demands for enlargement of display size and/or tandem-structure photovoltaics having sensitivity in a wide range of spectral region of the sun. Among several kinds of TCO materials, tin-doped In_2O_3 (ITO) has been widely used as transparent electrodes for flat panel displays and thin-film solar cells, because ITO films having high transparency to visible light and low resistivity can be easily fabricated at relatively low temperature, compared to other TCO materials such as SnO_2 or ZnO . Recently, high-mobility In_2O_3 based thin films on glass have been discovered by doping metals such as Mo,^{2–4} Ti,⁵ and W,⁶ and demonstrated as a transparent electrode for solar cells having sensitivity in visible to near infrared (NIR) wavelength region.⁷ These reports have been received with enthusiasm due to their exceptionally high carrier mobility under carrier density larger than 10^{20} cm^{-3} , $130 \text{ cm}^2/\text{V s}$ and $2.6 \times 10^{20} \text{ cm}^{-3}$ for $\text{In}_2\text{O}_3:\text{Mo}$,² $83 \text{ cm}^2/\text{V s}$ and $2.9 \times 10^{20} \text{ cm}^{-3}$ for $\text{In}_2\text{O}_3:\text{Ti}$,⁵ and $104 \text{ cm}^2/\text{V s}$ and $2.0 \times 10^{20} \text{ cm}^{-3}$ for $\text{In}_2\text{O}_3:\text{W}$ (Ref. 6) on glass. These values of mobility are factors of 2–3 greater than those measured in ITO. However, not only the best doping elements but also the origins of the high mobility themselves have not been cleared yet.

In the case of TCO, the electric properties of TCO especially grown on glass at low temperature strongly depend on the growth method and/or growth conditions, because carriers in TCO are generated by creation of intrinsic donors by lattice defects (oxygen vacancies⁸ or interstitial metals⁹) or extrinsic dopants, and, in reality, both doping mechanisms occur simultaneously. Therefore, in order to know the effects of dopants on the electric properties, single crystals or epilayers, having small numbers of intrinsic donors, are one of the model systems. Recently, we have succeeded in the fabrication of high-mobility ($89\text{--}110 \text{ cm}^2/\text{V s}$) In_2O_3 heteroepitaxial layers with reduced carrier density [$(6.0\text{--}7.8) \times 10^{18} \text{ cm}^{-3}$].¹⁰ In this letter, the impacts of Zr doping to the In_2O_3 epilayers on the optical and electric properties are described and compared to those of Sn-doped In_2O_3 epilayers grown under the same conditions.

Approximately 250-nm-thick $\text{In}_{2-2x}\text{Me}_{2x}\text{O}_3$ (Me:Sn, Zr) epilayers ($x=0, 0.003, 0.01, 0.02, 0.05$) were grown on (111) yttria-stabilized zirconia (YSZ) substrates using combinatorial pulsed laser deposition system¹¹ by ablating In_2O_3 and $\text{In}_{1.8}\text{Me}_{0.2}\text{O}_3$ (Me:Sn, Zr) ceramic targets. The detailed procedures of depositing the films using two targets are written elsewhere.^{12,13} The fluence and repetition rate of KrF excimer laser were $100 \text{ mJ}/\text{cm}^2$ and 5 Hz, respectively. The substrate temperature and oxygen pressure during growth were 650°C and 3×10^{-2} Torr, respectively. The metal compositions of the films were analyzed by the electron dispersive x-ray analysis. The crystal structure was analyzed by x-ray diffraction (XRD). Transmittance and reflectance spectra were measured by ultraviolet/visual/NIR spectrophotometers. Electrical resistivity and Hall mobility were measured for the films using van der Pauw's method.

Figure 1 shows XRD θ - 2θ profiles for $\text{In}_{1.9}\text{Sn}_{0.1}\text{O}_3$ and $\text{In}_{1.9}\text{Zr}_{0.1}\text{O}_3$ films on (111) YSZ substrates. All the $\text{In}_{2-2x}\text{Me}_{2x}\text{O}_3$ (Me:Sn, Zr) films showed (111) orientation growth and no other impurity phases were observed, indicating that the films were grown epitaxially and solid solution occurred in this composition range. From the XRD θ - 2θ and ω profiles (data not shown) of the films, no drastic change in axis length and no deterioration of the crystallinity with x were observed in $\text{In}_{2-2x}\text{Zr}_{2x}\text{O}_3$. The results are probably due to the similar sizes of ionic radii, i.e., In^{3+} : 80.0 pm, Sn^{4+} : 69.0 pm, and Zr^{4+} : 72.0 pm.

Figures 2(a) and 2(b) are transmittance and reflectance spectra of the $\text{In}_{2-2x}\text{Me}_{2x}\text{O}_3$ (Me:Sn, Zr) epilayers on YSZ substrates, respectively. In $\text{In}_{2-2x}\text{Sn}_{2x}\text{O}_3$, a large decrease in

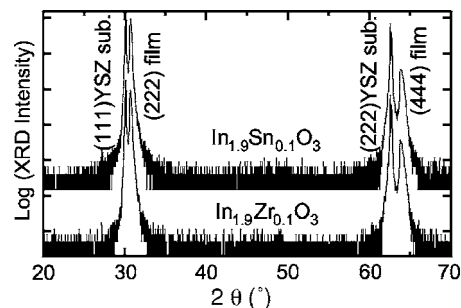


FIG. 1. XRD θ - 2θ profiles for $\text{In}_{1.9}\text{Sn}_{0.1}\text{O}_3$ and $\text{In}_{1.9}\text{Zr}_{0.1}\text{O}_3$ films on (111) YSZ substrates.

^{a)}Electronic mail: t-koida@aist.go.jp

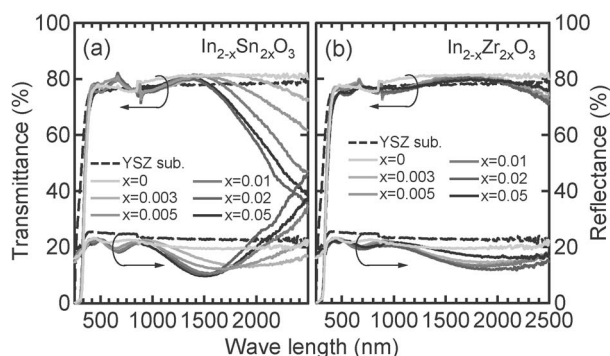


FIG. 2. Transmittance and reflectance spectra of $\text{In}_{2-x}\text{Sn}_{2x}\text{O}_3$ (a) and $\text{In}_{2-x}\text{Zr}_{2x}\text{O}_3$ (b) epilayers on YSZ substrates. The spectra of YSZ substrates are also shown as dotted lines.

transmittance and a large increase in reflectance in NIR wavelength region were observed in the composition range over $x=0.005$ due to the free-carrier absorption, while only slight changes were observed in $\text{In}_{2-x}\text{Zr}_{2x}\text{O}_3$. These results reflect low carrier density and high mobility in $\text{In}_{2-x}\text{Zr}_{2x}\text{O}_3$ at Zr composition less than 0.02, compared to $\text{In}_{2-x}\text{Sn}_{2x}\text{O}_3$ as described below.

Figures 3 shows the electrical resistivity, carrier density, and Hall mobility of the $\text{In}_{2-x}\text{Me}_{2x}\text{O}_3$ (Me:Sn, Zr) epilayers as a function of x . The dotted line is the expected carrier density assuming that all the Me^{4+} ions substitute the In^{3+} sites and generate one electron per Me. The carrier densities of the $\text{In}_{2-x}\text{Zr}_{2x}\text{O}_3$ epilayers followed the dotted line in the composition range from 0 to 0.005, reflecting that Zr behaves as good donor impurities like Sn, i.e., one Me^{4+} substitutes for one In^{3+} . Simultaneously, the values of mobility of the $\text{In}_{2-x}\text{Zr}_{2x}\text{O}_3$ epilayers are much larger than that of the pure In_2O_3 , which was in contrast to the case of $\text{In}_{2-x}\text{Sn}_{2x}\text{O}_3$ epilayers. Accordingly, the compositions of Zr, at which the resistivities showed the lowest values, were smaller than that of Sn.

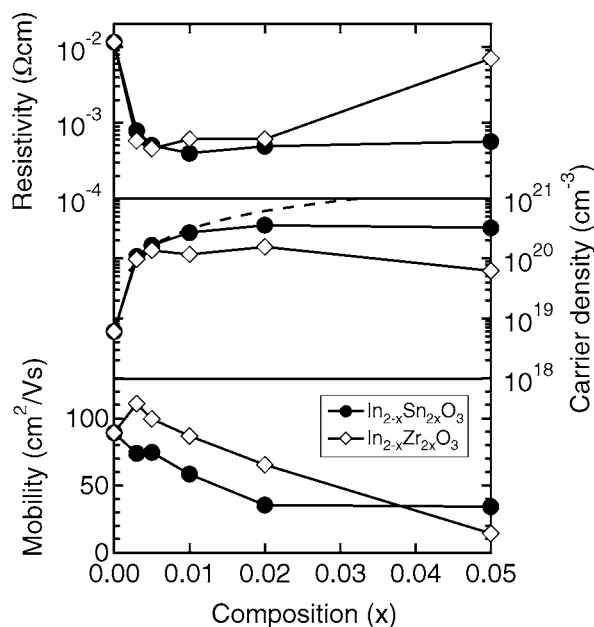


FIG. 3. Resistivity, carrier density, and mobility of $\text{In}_{2-x}\text{Me}_{2x}\text{O}_3$ (Me:Sn, Zr) epilayers as a function of composition (x). The dotted line denotes the expected carrier density assuming that all the Me^{4+} ions substitute the In^{3+} sites and generate one electron per Me.

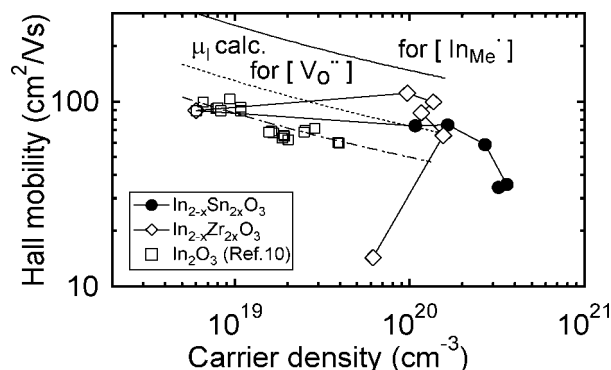


FIG. 4. Hall mobility of $\text{In}_{2-x}\text{Me}_{2x}\text{O}_3$ (Me:Sn, Zr) epilayers as a function of carrier density, and each symbol is connected by lines from $x=0$ to $x=0.05$. The values of our undoped In_2O_3 epilayers (after Ref. 10) are also shown. The solid and dotted lines are the calculated mobilities due to ionized impurities assuming that the conducting carriers originate entirely from singly and doubly charged impurities, respectively.

One of the origins of the high mobility in $\text{In}_{2-x}\text{Zr}_{2x}\text{O}_3$ seems to be reduced impurity scattering centers, since the mobility is determined by the scattering of electrons from ionized or neutral impurities (intrinsic lattice defects or extrinsic dopants) for high charge carrier concentrations. In order to discuss it, Fig. 4 summarizes the relationship between Hall mobility and carrier density for the $\text{In}_{2-x}\text{Me}_{2x}\text{O}_3$ (Me:Sn, Zr) epilayers. Each symbol is connected by lines from $x=0$ to $x=0.05$. Our undoped In_2O_3 epilayers fabricated in the same growth chamber under various oxygen pressures and growth temperatures¹⁰ are also shown. The dotted and solid lines are the calculated mobilities due to ionized impurities (μ_I) assuming that the conducting carriers originate entirely from doubly charged oxygen vacancies and singly charged Me^{4+} , respectively. The details of the expressions for μ_I are written elsewhere.¹⁰ Briefly, the expressions derived by Dingle¹⁴ were used in this study to express the μ_I for degenerate semiconductors having parabolic band structures, since carrier densities of $\text{In}_{2-x}\text{Zr}_{2x}\text{O}_3$ epilayers were from 6.0×10^{18} to $1.6 \times 10^{20} \text{ cm}^{-3}$, and the effects of the nonparabolicity of the conduction band^{15,16} were observed strikingly for carrier concentrations over approximately $1 \times 10^{20} \text{ cm}^{-3}$.^{17,18} Also, the values of effective mass and low-frequency relative permittivity were taken as $0.3m_0$ and 9,¹⁹ respectively.

All the undoped In_2O_3 epilayers seem to align on a line as shown by a dashed line. The slopes of the dotted and dashed lines are in good agreement with some discrepancies in the values of mobility, indicating that mobility of the undoped epilayers is dominated by the scattering of electrons from doubly charged oxygen vacancies and small number of neutral or ionized scattering centers, which might have originated from impurities in the ceramic targets and/or the growth chamber. With introducing Sn or Zr to the In_2O_3 , the mobility exceeded the theoretical value dominated by scattering from doubly charged ions (dotted line) and approached the value dominated by scattering from singly charged ions (solid line) at a given carrier density. Note that the values of mobility in $\text{In}_{2-x}\text{Zr}_{2x}\text{O}_3$ at Me concentrations of 0.3–0.5 at. % were much higher than those of $\text{In}_{2-x}\text{Sn}_{2x}\text{O}_3$ having the same carrier density. However, further increase in x resulted in the saturation of carrier density with a decrease in mobility, and the phenomena appeared at lower x in $\text{In}_{2-x}\text{Zr}_{2x}\text{O}_3$. These results can be explained as follows. For

doped epilayers, mobility is supposed to be dominated by the scattering of electrons from singly charged Me, multicharged ions including oxygen vacancies and interstitials, and/or neutral defects which consist of Me and the additional oxygen.²⁰ The effects of scattering from the multicharged ions and/or defects on the mobility in $\text{In}_{2-2x}\text{Zr}_{2x}\text{O}_3$ are smaller than those in $\text{In}_{2-2x}\text{Sn}_{2x}\text{O}_3$ at Me compositions less than 1 at.%. Further increase in Me composition led to an increase in electrically inactive Me in In_2O_3 , which does not generate free carriers. The electrically inactive Me in In_2O_3 lattice is considered to have negative effects on electrical conductivity in terms of producing neutral scattering centers. The mechanisms of the scattering of free carriers and/or the donor compensation in $\text{In}_{2-2x}\text{Me}_{2x}\text{O}_3$ have not been completely clarified yet, however, the difference of interactions between substitutional Me and oxygen (including oxygen vacancies and interstitial oxygens) may influence them.

In summary, Zr-doped In_2O_3 is found to be a superior transparent conductive oxide in transparency in near infrared wavelength region and Hall mobility compared to Sn-doped In_2O_3 . The optical transparency is high in a wide spectral range from 400 to at least 2500 nm. The carrier density increased with Zr content, and one carrier is generated per added Zr between 0 and 0.5 at.%. Maximum mobilities of the films at Zr concentrations of 0.3–0.5 at.% are over $100 \text{ cm}^2/\text{Vs}$ and corresponding carrier densities are approximately $1 \times 10^{20} \text{ cm}^{-3}$. The experimental results are explained by a reduction of a number and/or effects of multicharged and neutral scattering centers of electrons in Zr-doped In_2O_3 . These materials have the potential to replace ITO to improve optoelectronic devices such as thin-film solar

cells and photodetectors having sensitivity in the near infrared wavelength region.

- ¹For example, see T. Minami, MRS Bull. **25**, 38 (2000).
- ²Y. Meng, X. Yang, H. Chen, J. Shen, Y. Jiang, Z. Zhang, and Z. Hua, Thin Solid Films **394**, 219 (2001).
- ³Y. Yoshida, T. A. Gessert, C. L. Perkins, and T. J. Coutts, J. Vac. Sci. Technol. A **21**, 1092 (2003).
- ⁴C. Warmstrong, Y. Yoshida, D. W. Readey, C. W. Teplin, J. D. Perkins, P. A. Parilla, L. M. Gedvilas, B. M. Keyes, and D. S. Ginley, J. Appl. Phys. **95**, 3831 (2004).
- ⁵M. F. A. M. van Hest, M. S. Dabney, J. D. Perkins, D. S. Ginley, and M. P. Taylor, Appl. Phys. Lett. **87**, 032111 (2005).
- ⁶P. F. Newhouse, C.-H. Park, D. A. Keszler, J. Tate, and P. S. Nyholm, Appl. Phys. Lett. **87**, 112108 (2005).
- ⁷J. A. A. Selvan, Y. Li, S. Guo, and A. E. Delahoy, *Proceedings of the 19th European PVSEC, Paris, France* (WIP, Munich and ETA, Florence, 2004), pp. 1346–1351.
- ⁸J. H. W. de Wit, J. Solid State Chem. **20**, 143 (1977).
- ⁹A. J. Rosenberg, J. Phys. Chem. **64**, 1143 (1960).
- ¹⁰T. Koida and M. Kondo, J. Appl. Phys. **99**, 123703 (2006).
- ¹¹T. Ohnishi, D. Komiyama, T. Koida, S. Ohashi, C. Stauter, H. Koinuma, A. Ohtomo, M. Lippmaa, N. Nakagawa, M. Kawasaki, T. Kikuchi, and K. Omote, Appl. Phys. Lett. **79**, 536 (2001).
- ¹²Y. Matsumoto, M. Murakami, Z. Jin, A. Ohtomo, M. Lippmaa, M. Kawasaki, and H. Koinuma, Jpn. J. Appl. Phys., Part 2 **38**, L603 (1999).
- ¹³T. Koida, T. Wakisaka, K. Itaka, H. Koinuma, and Y. Matsumoto, Appl. Phys. Lett. **81**, 4955 (2002).
- ¹⁴R. B. Dingle, Philos. Mag. **46**, 831 (1955).
- ¹⁵R. T. Bate, R. D. Baxter, F. J. Reid, and A. C. Beer, J. Phys. Chem. Solids **26**, 1205 (1965).
- ¹⁶T. Pisarkiewicz, K. Zakrzewska, and E. Leja, Thin Solid Films **174**, 217 (1989).
- ¹⁷Y. Ohhata, F. Shinoki, and S. Yoshida, Thin Solid Films **59**, 255 (1979).
- ¹⁸A. K. Kulkarni and S. A. Knickerbocker, J. Vac. Sci. Technol. A **14**, 1709 (1996).
- ¹⁹I. Hamberg and C. G. Granqvist, J. Appl. Phys. **60**, R123 (1986).
- ²⁰N. Yamada, I. Yasui, Y. Shigesato, H. Li, Y. Ujihira, and N. Nomura, Jpn. J. Appl. Phys., Part 1 **38**, 2856 (1999).